

## Ebullition events monitored from northern peatlands using electrical imaging

Nicholas Kettridge,<sup>1</sup> Andrew Binley,<sup>1</sup> Sophie M. Green,<sup>2</sup> and Andy J. Baird<sup>3</sup>

Received 29 September 2010; revised 28 June 2011; accepted 8 July 2011; published 7 October 2011.

[1] Within northern peatlands, ebullition is potentially an important mechanism for the transport of methane (CH<sub>4</sub>) to the atmosphere. We applied electrical imaging to characterize the buildup and ebullition of biogenic gas bubbles in a spatially explicit manner. Ebullition events were monitored from a range of different peat types, with and without a vascular plant cover, under different meteorological conditions. Weekly changes in bulk electrical conductivity ( $\sigma$ ) were analyzed, during which variations in pore water conductivity had only a small effect on  $\sigma$ . Bulk ebullition losses from the peat cores were independently measured using Mariotte regulators. The largest ebullition events were found to be spatially diffuse: the gas was released from a large volume of peat. We used a measure of the roughness of the electrical images to characterize the magnitude of gas bubble movement within each peat core. Our results show that small variations in air temperatures of 3°C and variations in peat type between different microhabitats have a statistically significant influence on gas bubble dynamics.

**Citation:** Kettridge, N., A. Binley, S. M. Green, and A. J. Baird (2011), Ebullition events monitored from northern peatlands using electrical imaging, *J. Geophys. Res.*, 116, G04004, doi:10.1029/2010JG001561.

### 1. Introduction

[2] Northern peatlands represent important stores of carbon, accounting for approximately one third of the global soil carbon pool [Gorham, 1991]. Currently, northern peatlands are net sinks of atmospheric CO<sub>2</sub> but large sources of methane (CH<sub>4</sub>). CH<sub>4</sub> is a potent greenhouse gas, and variations in its flux under changing climatic conditions are likely to dominate alterations to the climatic forcing effect of northern peatlands in the short to medium term (10–100 years) [Frolking *et al.*, 2006]. However, there remains considerable uncertainty about how methane is stored in and released from northern peatlands and how the magnitude of this flux is likely to vary with changing climatic conditions.

[3] Within northern peatlands, CH<sub>4</sub> is produced under anaerobic conditions (beneath the water table) and is transported to the atmosphere via diffusion through the peat matrix, plant-mediated transport and ebullition (steady and episodic). Episodic ebullition is the sporadic movement of free-phase gas bubbles through the peat profile and is the focus of this paper. The proportion of the total CH<sub>4</sub> flux from northern peatlands transported via ebullition is uncertain, with current estimates ranging from 18 to 89% [Christensen *et al.*, 2003; Lansdown *et al.*, 1992]. The mechanism by which methane is transported through peat is

important because it controls the rate at which methane reaches the aerobic zone where it is in part oxidized to produce CO<sub>2</sub>, a less potent greenhouse gas [Granberg *et al.*, 1999]. The buildup and release of biogenic gas bubbles results in strong temporal variations in the CH<sub>4</sub> flux of up to two orders of magnitude over periods of minutes to hours [Tokida *et al.*, 2007]. Such short-term, high-flux, events may overwhelm the oxidation potential of the aerobic zone, substantially increasing the proportion of CH<sub>4</sub> reaching the atmosphere. Furthermore, the buildup and release of biogenic gas bubbles also has a number of indirect effects on the carbon balance of northern peatlands, influencing biogeochemical function [Strack *et al.*, 2005], hydraulic conductivity [Beckwith and Baird, 2001], hydraulic gradients [Kellner *et al.*, 2004] and peat buoyancy [Strack *et al.*, 2006].

[4] Attempts to simulate ebullition are limited by difficulties in measuring the dynamics of bubbles within peat. To date, most measurements have been of bubble loss from the peatland surface, not of the bubble dynamics within the peat. Ebullition may be observed using gas traps (laboratory) [Baird *et al.*, 2004] and flux funnels (field) [Strack *et al.*, 2005]. Step increases in either the peat moisture content [Comas *et al.*, 2008] or CH<sub>4</sub> concentrations during flux chamber measurements [Green and Baird, 2011] also provide information on episodic ebullition events. Ebullition models have been constructed based on data obtained from these measurement methods: an inverted sandpile-analogy model has been developed to describe the episodic/cyclical nature of ebullition observed from gas traps and flux funnels [Coulthard *et al.*, 2009] and a threshold gas-entrapment model [Kellner *et al.*, 2006] has been developed from gas

<sup>1</sup>Lancaster Environment Centre, Lancaster University, Lancaster, UK.

<sup>2</sup>Department of Earth and Environmental Science, The Open University, Milton Keynes, UK.

<sup>3</sup>School of Geography, University of Leeds, Leeds, UK.

contents monitored using moisture probes [e.g., Baird *et al.*, 2004]. Based on bulk measures of gas entrapment and ebullition, such models effectively make guesses about the dynamics of bubbles within the peat: gas traps/funnels and chambers provide a measure of the ebullition flux from the peat below, while moisture probes provide a bulk measure of the change in gas content from the volume of peat measured. In comparison, geophysical measurement techniques have the potential to provide a spatially distributed and detailed estimate of peat moisture content and offer the opportunity both to evaluate the current ebullition models and to provide the foundation for the next generation of such models.

[5] Three separate geophysical measurement methods have, to date, been used to provide details of the spatial distribution of entrapped gas within peat: ground penetrating radar [Comas and Slater, 2007], electrical imaging [Slater *et al.*, 2007] and X-ray computed tomography [Kettridge and Binley, 2008]. These methods have generally been used to provide a single spatially distributed measure of the entrapped gas content at a range of spatial scales [Strack and Mierau, 2010; Kettridge and Binley, 2008]. However, without repeat measurements of the entrapped gas content, the ebullition dynamics of a peat soil cannot be evaluated. For example, regions within the peat profile with higher entrapped gas contents cannot be directly classified as contributing to the ebullition flux. A region of higher gas content may represent a stable zone of entrapped biogenic gas within the peat, while regions of lower gas content may have a high “turnover” of bubbles.

[6] Slater *et al.* [2007] and Comas and Slater [2007] provide the only spatially distributed repeat monitoring of peat moisture content using geophysical methods. Slater *et al.* [2007] and Comas and Slater [2007] monitored the biogenic gas content within near-surface peat blocks using electrical resistivity and ground penetrating radar (GPR), respectively. However, these experiments were designed primarily to evaluate the potential of the two methods and were conducted on individual peat blocks; no experimental replications were used, nor were measurements performed on samples of differing peat type under varying meteorological conditions. We sought to extend the work of Comas and Slater [2007] and conducted replicate experiments under different meteorological conditions, on different peat types, with different plant communities, to elucidate how these factors affect the bubble dynamics of peat. Our rationale for looking at these factors is given below.

[7] *Meteorological conditions:* Methanogenesis is exponentially related to peat temperatures [Dunfield *et al.*, 1993]. Higher rates of CH<sub>4</sub> production under warmer temperatures have been shown to enhance the ebullition flux from peat [Waddington *et al.*, 2009]. We aim to investigate how temperature affects bubble dynamics within peat, both in terms of rates of bubble formation but also in terms of bubble movement and loss.

[8] *Peat type:* The entrapment and loss of biogenic gas bubbles is spatially variable [Strack and Mierau, 2010]. It has been hypothesized that differences in the buildup and loss of biogenic gas bubbles is associated with variations in peat physical properties [Kettridge and Binley, 2011]. Peats with lower porosities and smaller, more tortuous, pore networks are more likely to trap biogenic gas bubbles [Kettridge and Binley, 2011]. Consequently, we further aim

to monitor differences in the entrapment and ebullition of biogenic gas bubbles in a range of different peat types to characterize their control on bubble dynamics and ebullition.

[9] *Vascular plant cover:* It has been hypothesized that the presence of vascular plants can both enhance and reduce the buildup of biogenic gas bubbles in near-surface peat. Vascular plants such as sedges allow the diffusion of oxygen down into the anaerobic zone, reducing CH<sub>4</sub> production and enhancing methanotrophy [Ström *et al.*, 2005; Waddington *et al.*, 1996], the combined effect of which should be a reduction in rates of net CH<sub>4</sub> production and reductions in rates of bubble formation, growth, and loss. In contrast, root exudates from vascular plants are a substrate for methanogens; therefore, vascular plants may increase rates of CH<sub>4</sub> production [Joabsson *et al.*, 1999; Ström *et al.*, 2003; Waddington *et al.*, 1996]. Vascular plants also allow the diffusion of CH<sub>4</sub> from the anoxic zone to the atmosphere, providing an additional transport pathway for CH<sub>4</sub> [Thomas *et al.*, 1996]; potentially reducing the methane concentration within the anoxic zone and thus reducing the formation of biogenic gas bubbles. It is unclear whether or not these competing effects cancel. Therefore, another aim of our experiment was to provide an evaluation of spatially distributed differences in the buildup and loss of biogenic gas bubbles in peat cores with and without a vascular plant cover.

[10] We focus on the analysis of entrapped biogenic gas bubbles within the near-surface peat where the availability of labile carbon leads to high rates of CH<sub>4</sub> and CO<sub>2</sub> production. We do not consider the buildup of biogenic gas bubbles deeper within the peat profile [cf. Dinel *et al.*, 1988; Glaser *et al.*, 2004]. The electrical imaging method used in our study is first outlined; its use for monitoring bubble dynamics is then justified.

## 2. Electrical Imaging

[11] Electrical imaging reconstructs the 2-D or 3-D distribution of the bulk electrical conductivity ( $\sigma$ ) of a medium from a large number of four-electrode resistance measurements (resistance being the reciprocal of conductance). Two electrodes are used to produce an electrical circuit through the peat and a further two are used to measure the potential difference that results from the current injection [for more information, see Binley and Kemna, 2005]. The bulk electrical conductivity is dependent on the physical and chemical properties of the porous medium (e.g., porosity, degree of saturation ( $S_w$ ), cation exchange capacity) and the electrical conductivity of the pore fluid ( $\sigma_w$ ). Spatial variations in peat  $S_w$  cannot be accurately obtained from a single electrical image because of the number of competing factors that influence  $\sigma$  and because variations in  $S_w$  due to gas entrapment within the peat are unlikely to have a dominant control on  $\sigma$  [Slater *et al.*, 2007]. However, by performing a time-lapse inversion [cf. Daily *et al.*, 2004] and by monitoring changes in  $\sigma$  over time, an accurate measure of changes in  $S_w$  can be obtained [e.g., Binley *et al.*, 2002].

[12] Comas and Slater [2004] provide the only detailed investigation to date of the electrical properties of peat, quantifying the relationship between the pore water conductivity and the bulk electrical conductivity of four separate peat samples. However, these relationships, developed for deep peats (>1.0 m deep), were shown by Slater *et al.*

[2007] to provide a poor representation of the electrical properties of near-surface (<0.2-m deep), poorly decomposed peat. These empirical relationships were also derived at relatively high pore water electrical conductivities (100–10,000  $\mu\text{S cm}^{-1}$ ). The pore water conductivity of the near-surface peat at the sites studied here (see section 4 below) was <100  $\mu\text{S cm}^{-1}$ . The relationships developed by *Comas and Slater* [2004] at higher conductivities are unlikely to be reliable for our lower conductivities. In addition, the effect of variations in  $S_w$  has not been quantitatively characterized for peat samples. *Slater et al.* [2007] approximated the degree of saturation of the peat by applying Archie's law, a relationship derived originally from sedimentary rocks. This relationship was parameterized by *Slater et al.* [2007] by comparing the variations in electrical resistivity monitored during their experiment with the degree of saturation of a separate adjacent peat sample measured using GPR. *Slater et al.* [2007] explicitly recognized the need for an improved characterization of the relationship between  $\sigma$  and  $S_w$ . Therefore, to enable bubble dynamics and ebullition events to be characterized accurately using electrical imaging, we aimed to develop empirical relationships between  $\sigma$  and  $S_w$  for a range of different peat types.

[13] In comparison to electrical imaging, GPR and X-ray computed tomography provide a more explicit measure of peat moisture content. Variations in the dielectric permittivity measured by GPR and the linear attenuation measured by X-ray CT are both controlled principally by the volumetric moisture content ( $\theta$ ) of the peat [*Kellner and Lundin*, 2001; *Kettridge and Binley*, 2008]. However, the difficulty in automating GPR measurements prevents the approach from being applied to the repeat monitoring of spatial variations in peat  $\theta$  on a large number of peat cores. In addition, the small size of the samples that can be imaged by micro X-ray CT scanners [*Kettridge and Binley*, 2008] and the limited access to larger medical scanners prevents X-ray computed tomography from being used on samples that are large enough to be representative of field conditions. In comparison, if variations in the pore water electrical conductivity are either small or can be characterized adequately, electrical resistivity is a fast, relatively inexpensive, non-invasive method of monitoring the 3-D spatial variation in peat  $S_w$  [*Slater et al.*, 2007]. The approach can be applied to monitor spatial variations in the entrapped gas content within a large number of representative peat samples without movement or disturbance of the samples.

### 3. Experimental Design

[14] Three separate experiments were conducted, entitled calibration experiment (CE), experiment 1 (E1) and experiment 2 (E2). CE aimed to develop an appropriate relationship between  $\sigma$  and  $S_w$  for the range of peat types studied in E1 and E2. E1 applied electrical imaging to monitor the buildup and ebullition of biogenic gas bubbles within incubated peat cores of three different peat types. E1 investigated whether electrical imaging can identify the spatial distribution in the buildup and ebullition of gas bubbles. In addition, E1 aimed to identify the origin of escaping bubbles, the movements of bubbles within peat cores, and the control of meteorological conditions and peat type on these bubble dynamics. E2 monitored the ebullition

of biogenic gas bubbles within a single peat type in cores with and without a cover of vascular plants, under partially shaded and full light conditions, to characterize the importance of the competing controls of a vascular vegetation cover on methane ebullition. Under full light conditions, the comparison of bubble dynamics between peat cores with and without a vascular vegetation cover provides an indication of the combined effects of root exudates and rhizospheric oxidation on methane ebullition. Under shaded conditions, the same comparison helps reveal the effect of rhizospheric oxidation on methane ebullition. The passive transport of oxygen to the rhizosphere will be unaffected by the shaded conditions, while carbon fixation (and the production of root exudates) by vascular plants will be reduced [*Öquist and Svensson*, 2002; *Ström et al.*, 2003].

[15] Below, we first outline the collection of peat cores for use in CE, E1 and E2, before providing an overview of the three experiments.

### 4. Sample Collection

[16] Samples were obtained from two lowland raised bogs in the United Kingdom; Cors Fochno (52°31'0 N, 4°1'60 W) and Longbridge Muir (55°00'1 N, 3°27'29 W). Large areas of Cors Fochno remain relatively undisturbed and are characterized by the range of pool to hummock microhabitats found in many northern bogs. While large areas of Longbridge Muir have been damaged by extensive afforestation and deforestation, areas of the site have remained relatively undisturbed. A total of 28 peat samples, 0.2 m in diameter, 0.5 m in depth, were obtained from three different microhabitats within the undisturbed areas of these peatlands: (1) Longbridge Muir lawn, composed of *Sphagnum magellanicum* Brid. and *Calluna vulgaris* L. (Hull); (2) Longbridge Muir hollow, *Sphagnum capillifolium* (Ehrh.) Hedw. *Calluna vulgaris* L. (Hull); and (3) Cors Fochno hollow, composed of *Sphagnum pulchrum* (Lindb. ex Braithw.) Warnst. and White-beaked Sedge *Rhynchospora alba* (L.) Vahl. Samples were extracted using the method outlined by *Kettridge and Binley* [2010]. Polyvinyl chloride (PVC) cylinders of 0.2 m o.d. were placed on the peat surface and cut around with scissors to a depth of ~2 cm. Each PVC cylinder was then pushed gently down through the cut peat. The peat around the outside of the sample holder was then excavated to the base of the PVC cylinder. This process was repeated until the cylinder was fully installed to a depth of 0.5 m. The peat beneath the sample holder was then cut and the cylinder and peat lifted out of the peat. The peat sample was sealed within a plastic bag and the sample transported back to the laboratory. The properties of each sample and the experiment for which it was used are outlined in Table 1.

### 5. Laboratory Methods

#### 5.1. CE

[17] To calculate changes in peat  $S_w$  from measured variations in  $\sigma$ , a relationship was derived between  $\sigma$  and  $S_w$ . Peat cores 1–6 (Table 1) were sub-sampled using a calibration cylinder (Figure 1) following the method outlined by *Kettridge and Binley* [2010]. The calibration subsamples were 0.07 m in diameter and 0.07 m in length. Thirteen

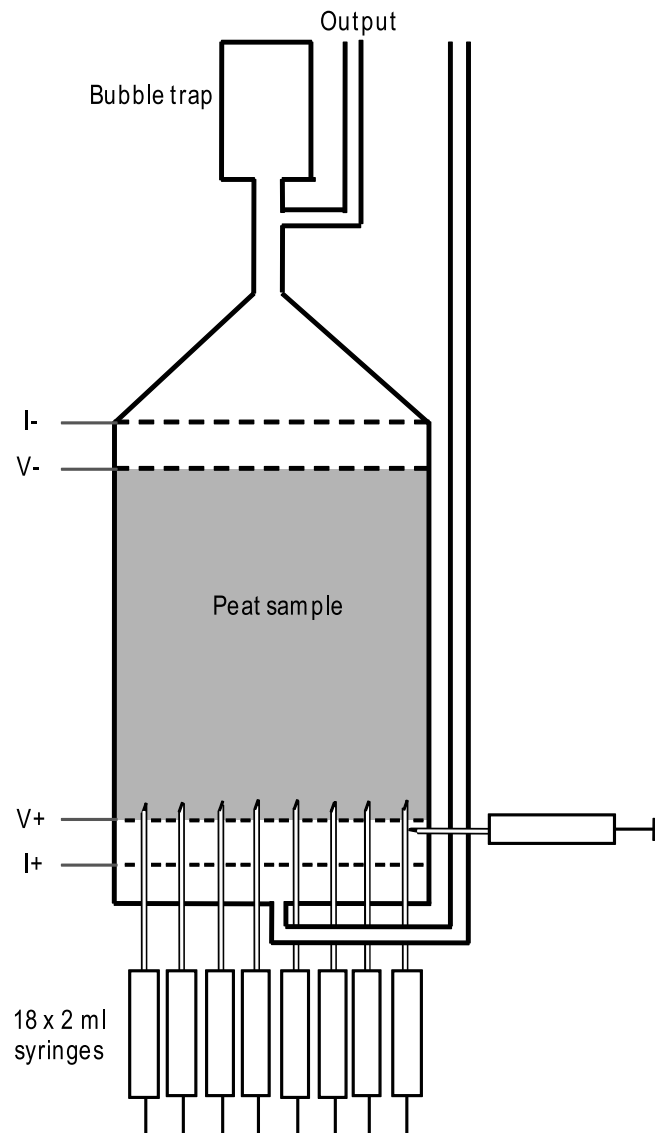
**Table 1.** Sample Numbers, the Experiment in Which the Samples Were Used, and the Associated Peat Type, With the Average *Sphagnum* Cover, Vascular Species, and Average Cover of Vascular Species Shown for Samples Incorporated Within E1 and E2<sup>a</sup>

Sample Number	Experiment	<i>Sphagnum</i> Species	Average Cover of <i>Sphagnum</i> Species	Vascular Species	Average Cover of Vascular Species
1–2	CE	<i>S. pulchrum</i>			
3–4	CE	<i>S. cuspidatum</i>			
5–6	CE	<i>S. magellanicum</i>			
7–10	E1	<i>S. pulchrum</i>	100%	<i>E. angustifolium</i> <i>R. alba</i>	<5% <5%
11–14	E1	<i>S. cuspidatum</i>	100%	<i>E. angustifolium</i> <i>R. alba</i>	5% <5%
15–18	E1	<i>S. magellanicum</i>	95%	<i>E. angustifolium</i> <i>E. vaginatum</i> <i>C. vulgaris</i> <i>V. myrtillus</i>	<5% <5% <5% <5%
19–23	E2	<i>S. cuspidatum</i>	95%	<i>N. ossifragum</i>	<5%
24–28	E2	<i>S. cuspidatum</i>	70%	<i>E. angustifolium</i> <i>E. vaginatum</i>	60% <5%

<sup>a</sup>Species abbreviated within the table are *Calluna vulgaris* (L.) Hull., *Eriophorum angustifolium* Honck., *Eriophorum vaginatum* L., *Narthecium ossifragum* (L.) Huds., *Rhynchospora alba* (L.) Vahl., *Sphagnum cuspidatum* Ehrh. ex Hoffm., *Sphagnum magellanicum* Brid., *Sphagnum pulchrum* (Lindb. ex Braithw.) Warnst., and *Vaccinium myrtillus* L.

subsamples were saturated from their base and subsequently flushed with 5 L of de-aired (boiled, temperature equilibrated) 0.06 M NaCl solution ( $\sim 80 \mu\text{S cm}^{-1}$ ; equivalent to the pore water conductivity of the incubated peat samples). After equilibration,  $\sigma$  was measured using an IRIS Syscal Pro (www.iris-instruments.com). Current was injected between two copper current electrodes at the base and top of each calibration subsample holder and voltage measured between the two stainless steel potential electrodes above and below the sample. The current electrodes consisted of circular disks perforated with nineteen 8-mm diameter holes to allow (1) insertion of syringe needles at the base of the sample holder (for bubble injection) and (2) escape of bubbles from the top into a gas trap. The potential electrode at the base of the peat sample was a fine mesh stainless steel circular disk that also allowed the insertion of the syringe needles. Above the sample the potential electrode was a coarse mesh disk that allowed free movement of gas bubbles.

[18] After the first measure of  $\sigma$  at saturation ( $\sigma_{sat}$ ), 0.1 mL of air was injected through each of the 18 syringe needles into the base of the peat sample. Following the injection, any gas that had emerged from the base of the sample was removed via a syringe installed on the side of the sample holder (Figure 1) and its total volume recorded. This buildup of gas below the base of the sample resulted from air traveling against the buoyancy force due to the increased pressure at the base of the peat sample. The degree of saturation of the peat was subsequently calculated from the peat porosity and the balance equation (the total trapped gas was equal to the total injected minus that removed from beneath the peat sample minus that captured in the gas trap above the sample). This process was repeated and a conductivity measurement taken between each air injection giving  $\sigma$  at different degrees of saturation,  $\sigma(S_w)$ . For three calibration samples this process was completed within an X-TEK Benchtop X-ray CT scanner. X-ray CT images of the peat sample were obtained before and after the injection of 2 mL (in 0.1 mL increments) through each of the 18 syringe needles, and the spatial distribution of the entrapped biogenic gas bubbles was obtained in accordance

**Figure 1.** Diagram of calibration cylinder.

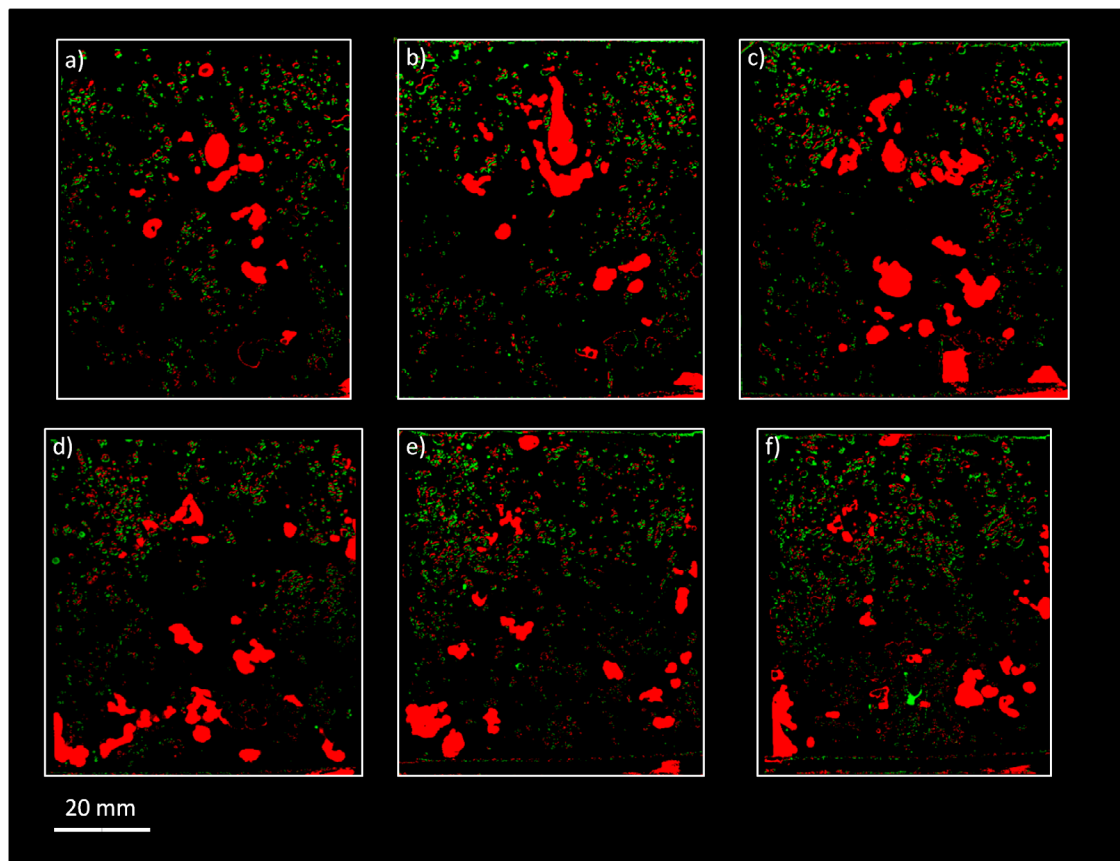


**Figure 2.** (a–f) Cross-sections through a cylindrical sample of *S. magellanicum* showing the change in classification of the sample (as either gas or water and peat) resulting from the injection of 144 ml of air. Black represents no change in the classification; red represents voxels classified as water or peat prior to the gas injection and as gas after the injection; and green represents voxels classified as gas prior to the gas injection and as water or peat after the injection.

with *Kettridge and Binley* [2008]. Differencing the CT images before and after the injection of air demonstrated that the injected gas bubbles were distributed throughout the peat core and were not retained in the peat in close proximity to the syringe needles (see, for example, Figure 2). The red regions in the image represent new gas bubbles that had been introduced into the peat profile. In addition to these large red regions, small changes in the classification of the sample are evident (these are more prevalent near the top of the sample). These changes in the image classification result from small movements of the peat between the repeat CT scan and are not as a result of the movement, loss or addition of gas.

## 5.2. Electrical Imaging of Peat Cores

[19] Electrical imaging was performed on the 0.2-m diameter, 0.5-m deep, peat cores. Each core was transferred from its field sample holder into an electrical imaging cylinder. These measurement cylinders had a total of ninety-six 8-mm diameter plate electrodes flush with the interior of the cylinder walls. Electrodes were arranged in eight rings of 12 electrodes at equal intervals around the sample holder. A single electrical image measurement of the peat sample consisted of 1219 independent four-electrode direct current (DC) measurements (normal and reciprocal measurements

obtained; 50V, 300 ms current injection) measured using a RESECS instrument ([www.geoserve.de](http://www.geoserve.de)). Measurements consisted of two configurations. In the first, current was injected between pairs of opposite electrodes within each electrode plane (each ring) and the potential was measured between all other pairs of opposite electrodes within the same plane. In the second, current was injected between pairs of neighboring electrodes in adjacent horizontal planes (adjacent rings), and the potential was measured between all other pairs of neighboring electrodes in the same two horizontal planes. This measurement scheme was shown in preliminary trials to provide good measurement sensitivity in the central region of the peat core. Ratio inversions, that identify the percentage change in  $\sigma$  between two electrical image measurements [cf. *Daily et al.*, 2004], were performed using the finite element based Occam's inversion code R3t (available from Andrew Binley, Lancaster University), outlined by *Binley and Kemna* [2005]. The ratio inversion included two discrete zones above and below the water table representing the saturated and unsaturated peat. Preliminary trials of the measurement setup demonstrated that the approach was capable of identifying zones of "artificial" gas, using a spherical balloon inflated to approximately 0.05 m in diameter within the center of a trial core of *S magellanicum* peat (data not shown for brevity).

These zones of gas were artificial and were not designed to replicate the spatial distribution of entrapped gas within peat cores.

[20] During incubation periods, resistance measurements were excluded (1) if the current injection of either the normal or the reciprocal measurement was less than 0.3 mA, (2) if the measured potential of either measurement was less than 20 mV, or (3) if the difference between normal and reciprocal measurements was greater than 5%. The average reciprocal error for each set of electrical measurements generally ranged between 0.3 and 0.5%. The weightings in the least squares objective function within the ratio inversions were calculated from the measured reciprocal errors. Reciprocal errors do not account for errors in the finite element model (notably, the discretization errors). However, such “modeling” errors were assumed to cancel out within ratio inversions and were excluded within this error analysis. Reciprocal errors provide a single estimate of the error of each data point [LaBrecque *et al.*, 1996]. We therefore simulated the total resistance error by pooling estimates of the reciprocal error and representing them by an empirical relationship in accordance with Koestel *et al.* [2008].

### 5.2.1. E1

[21] Cores 7 to 18 (four cores each of *S. pulchrum*, *S. cuspidatum* and *S. magellanicum* peat) were incubated for a period of 15 weeks within two Weiss-Gallenkamp Fitotron SGC097 CPX plant growth cabinets. This 15-week period was divided into two periods. During the first 10-week summer period, the temperature cycled between a day time and nighttime temperature of 15°C and 12°C, respectively. During the later 5-week autumn period, the temperature cycled between day time and nighttime temperatures of 12°C and 9°C, respectively. The water table within each core was maintained by Mariotte regulators at a constant depth beneath the peat surface similar to the water table depth observed (in the field) in the microhabitat from which each peat core was sampled (*S. magellanicum*, 0.06 m depth below the surface; *S. pulchrum*, 0.02 m; *S. cuspidatum* 0.01 m). In addition to controlling the water table position, the water level within the Mariotte regulators was recorded manually each weekday (Monday to Friday) and used to calculate bulk daily episodic ebullition loss from each peat core. Water flowed from the regulators to replace water lost from each peat core via evapotranspiration and to replace escaping biogenic gas bubbles. Water displaced by the buildup of entrapped gas was lost from the core via an overflow and did not recharge the Mariotte bottle. Evapotranspiration from each core was assumed to be constant between each day because the humidity, air temperature and photosynthetically active radiation (PAR) were set to unchanging diurnal cycles (for each season). In comparison, the loss of water due to episodic ebullition is, by definition, sporadic. Therefore, the water loss from the Mariotte regulators could be decomposed into two components, one of which represented episodic ebullition. Steady ebullition would have been treated as evapotranspiration from the Mariotte regulators (for further details, see S. M. Green and A. J. Baird, The importance of episodic ebullition methane losses from three peatland microhabitats—A controlled environmental study, 2011, unpublished manuscript).

[22] Single electrical image measurements (as noted above, each image comprised 1219 independent four-electrode

direct current (DC) readings) were taken each week on each peat core at the same time in the diurnal temperature cycle (at the midpoint of the daytime period). The temperature distribution is, therefore, constant between each electrical measurement of an individual peat core. Pore water samples were obtained each week from five or six depths (0.07, 0.14, 0.22, 0.30, 0.38, 0.46 m; depending on the microhabitat) after the electrical imaging measurements were performed and were used for estimation of the pore water electrical conductivity. Atmospheric pressure was logged with a van Essen Instruments “Diver” pressure transducer (accuracy of  $\sim\pm 0.5$  hPa and precision of  $\sim 0.2$  hPa;).

### 5.2.2. E2

[23] Five cores vegetated with *S. cuspidatum* and five cores with a cover of *S. cuspidatum* and the sedge *E. angustifolium* (C19–28) were incubated for an 18-week period under the summer meteorological conditions used in E1. The samples were incubated under full light conditions, as in E1 for a period of 6 weeks, followed by a partially shaded period for 6 weeks, followed by full light conditions for a further 6 weeks. Partially shaded conditions were based on a 45% reduction in PAR. Within cores C19–28 (with a sedge cover), the net ecosystem exchange was significantly lower during the partially shaded conditions compared to full light conditions ( $p = 0.001$ ) [Green and Baird, 2011]. This strongly suggests that root exudation during this period conditions was also strongly reduced. The difference in the vascular vegetation cover between samples 19–23 and 24–28 was maintained during the 18-week experiment period by regularly cutting any emerging vascular plants in cores 19–23. The additional experimental protocols were in accordance with E1.

## 6. Results

### 6.1. CE: Degree of Saturation Versus Conductivity Relationship

[24] Characterizing the relationship between  $\sigma(S_w)/\sigma_{sat}$  and  $S_w$  in moderately decomposed (von Post H4–10; von Post and Granlund [1926]) peat proved problematic. The injection of air caused a buildup of pressure within the syringe and at the base of the peat sample. Releasing the plunger caused the compressed air to re-expand within the syringe with little addition of gas to the peat sample. As the volume of injected air increased, the injected air was generally either forced beneath the peat sample or was transported through the sample in a single ebullition event with only a minimal increase in the entrapped gas content. As a result, it was only possible to obtain reliable relationships for relatively poorly decomposed peat near the peat surface (0.0–0.21 m depth). The relationship between  $\sigma(S_w)/\sigma_{sat}$  and  $S_w$  is shown in Figure 3 for the three peat types investigated here (13 samples in total) at  $S_w$  ranging from 0.89 to 1.0. While degrees of saturation below 0.89 have been reported within the literature [Baird *et al.*, 2004; Kellner *et al.*, 2006], such low saturations could not be artificially generated using the syringe method. This highlights the difficulties in artificially representing the distributed buildup of biogenic gas bubbles via a relatively small number of point sources.

[25] The relationship between  $\sigma(S_w)/\sigma_{sat}$  and  $S_w$  is non-linear and varies between different samples, and potentially between different peat types (Figure 3). The cause of the

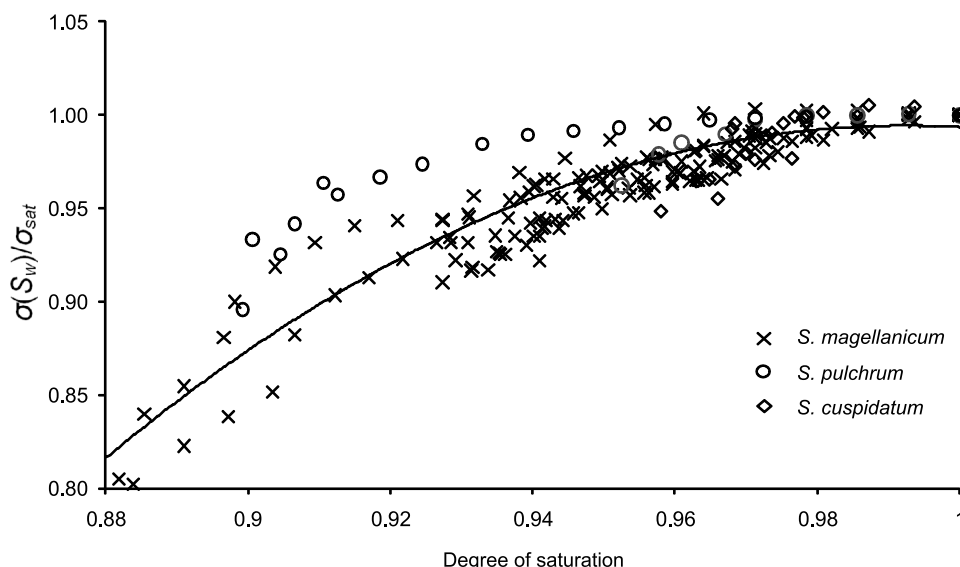


**Figure 3.** Ratio of degree of saturation to  $\sigma(S_w)/\sigma_{sat}$  at a range of peat saturations for samples of *S. magellanicum* (crosses), *S. pulchrum* (circles), and *S. cuspidatum* (diamonds).

small variation in  $\sigma(S_w)/\sigma_{sat}$  at near saturation is unclear. Small, well-distributed gas pockets may produce an insignificant alteration to  $\sigma(S_w)$  from its saturated value,  $\sigma_{sat}$ . Peat  $\sigma$  may only be reduced significantly when these small distributed gas pockets coalesce to produce larger bubbles that provide a more substantial barrier to the transfer of current through the peat.

[26] Variations in the relationship between  $\sigma(S_w)/\sigma_{sat}$  and  $S_w$  results principally from differences in the spatial organization of the entrapped gas. The injected gas was not uniformly distributed within the samples imaged with X-ray CT (Figure 2; see also section 5.1), although the entrapped gas was shown to be distributed throughout the sample away from the injection needles. Difference in the spatial arrangement of the entrapped gas may be greater between the peat types and even with different rates of gas generation, i.e., injected gas may be arranged differently from gas associated with the slow buildup associated with the anaerobic decay of peat. Further investigation is required in order to obtain a better understanding of the effect of variations in the spatial arrangement of the entrapped gas on the relationship between  $\sigma(S_w)/\sigma_{sat}$  and  $S_w$ . For simplicity, we represent the relationship for all the peat types using a second-order polynomial where:

$$\begin{aligned} \sigma(S_w)/\sigma_{sat} &= -14.09 S_w^2 + 27.97 S_w - 12.86 \\ r^2 &= 0.82, p < 0.01. \end{aligned} \quad (1)$$

This equation is applied to provide an indication of the magnitude of the variations in entrapped gas associated with measured  $\sigma(t)/\sigma(t_0)$ . The aim of this research is focused on identifying variations in the entrapped biogenic gas content in time and space, rather than obtaining exact quantification of the mass of gas trapped or lost. Therefore, equation (1) is not used to provide an accurate assessment of the volume of gas entrapped or lost from the incubated peat samples. While we recognize the limitation of the applied relationship, it is appropriate for the experimental aims of this

investigation and a significant improvement on the previously applied, poorly parameterized, Archie's equation (see section 2) [Slater *et al.*, 2007].

## 6.2. E1: Evaluation of Electrical Imaging Approach

[27] During each incubation experiment, measured  $\sigma$  varied temporally and spatially within each peat core. The spatial distribution in  $\sigma(t)/\sigma(t_0)$  within three peat cores of *S. magellanicum*, *S. cuspidatum* and *S. pulchrum* peat during experiment 1, at the end of the 15-week experiment period, are presented in Figure 4. Within the top 0.15 m of the peat profile,  $\sigma(t)/\sigma(t_0)$  is generally higher representing an increase in  $\sigma$  from its initial start value. In comparison, below a depth of 0.15 m,  $\sigma(t)/\sigma(t_0)$  reduces to approximately 0.85 of its initial value. All cores in both E1 and E2 showed this pattern. These temporal and spatial variations in  $\sigma(t)/\sigma(t_0)$  mirror the changes in the average  $\sigma_w$  observed during the experimental runs for all peat cores: Figure 5 shows  $\sigma_w$  increasing significantly at a depth of 0.07 m ( $p < 0.001$ ), showing no significant change at a depth of 0.14 m ( $p > 0.05$ ), and declining significantly at a depth of 0.30 m ( $p < 0.001$ ). Evaporation from the peat surface increased the ionic concentration in the near-surface. This evaporated water was replaced by deionized water, of a lower  $\sigma_w$ , generally to the lower portion of the peat profiles via the Mariotte regulators.

[28] The observed variations in  $\sigma_w$  are substantially smaller than those identified by Slater *et al.* [2007] (233 to 371  $\mu\text{S cm}^{-1}$  during their two-month experiment run). However, the variations in  $\sigma_w$  are the primary cause of the measured changes in  $\sigma$  during the experiment period. At a depth of 0.30 m, the average  $\sigma_w$  reduces from 72 to 60  $\mu\text{S cm}^{-1}$  over the 14-week measurement period (Figure 5c). In an unpublished paper, N. Kettridge and A. Binley show that for the range of peat types studied here,

$$\sigma = 0.67 \sigma_w + 33.0. \quad (2)$$

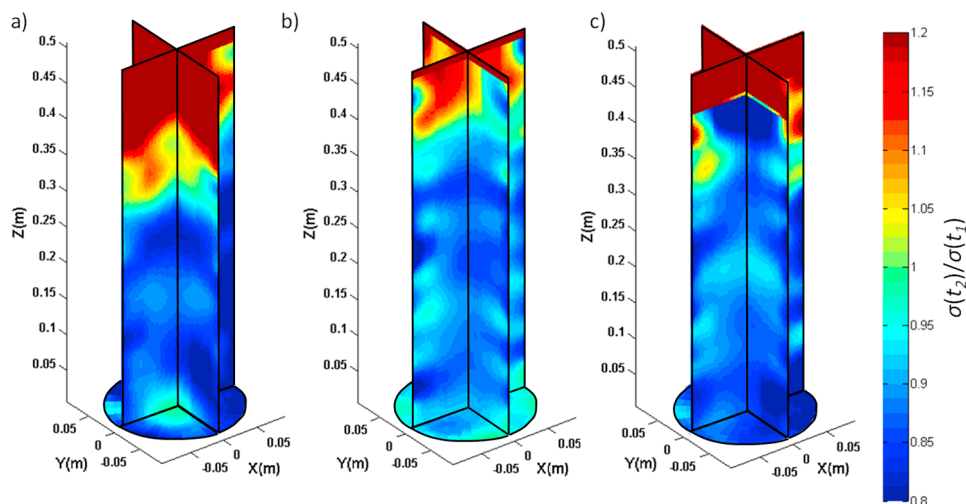


**Figure 4.** Measurements of  $\sigma(t)/\sigma(t_0)$  obtained after 14 weeks of incubation in experiment 1 for samples of (a) *S. pulchrum*, (b) *S. cuspidatum*, and (c) *S. magellanicum*.

In accordance with equation (2), this decline in  $\sigma_w$  alone would result in a  $\sigma(t)/\sigma(t_0)$  of 0.90 at a depth of 0.30 m, compared to the measured average of 0.85. Variations in  $S_w$  therefore have a second-order effect on  $\sigma(t)/\sigma(t_0)$ .

[29] Due to the controlled nature of the experimental conditions, temporal variations in  $\sigma_w$  would have been gradual, with no abrupt or sudden changes. Therefore, to estimate the uncertainty in the measured  $\sigma_w$ , third-order polynomials were fitted to the variation in measured  $\sigma_w$  with time at each measurement location. If it is assumed that the gradual variation in  $\sigma_w$  can be adequately represented by a third-order polynomial, the residuals of this relationship will provide a conservative estimate of the error in the measurement of  $\sigma_w$ . For all  $\sigma_w$  measurements, this gives a root mean square error of  $10.3 \mu\text{S cm}^{-1}$ . Assuming a degree of saturation of 0.95, a porosity of 0.95 and a  $\sigma_w$  of  $57.9 \mu\text{S cm}^{-1}$  (the average measured  $\sigma_w$ ), the uncertainty in the measured gas content equals  $\pm 0.06$ . Given the maximum expected variation in gas content during the incubation periods is 0.15 [Baird et al., 2004; Kellner et al., 2006], the buildup of gas within each core cannot be confidently back calculated from measured variations in  $\sigma(t)/\sigma(t_0)$ . In addition, the electrical imaging measurements provide a 3-D spatially distributed measurement of  $\sigma$ . Without installing a large number of probes, which would alter significantly the system being measured,  $\sigma_w$  can only be measured in 1-D at a low spatial resolution through the peat profile.

[30] While monitoring the temporal buildup of biogenic gas may prove problematic, electrical imaging can be applied to identify ebullition events. Temporal variations in  $\sigma$  associated with variations in  $\sigma_w$  are expected to occur slowly over the course of the incubation period. For example, at a depth of 0.07 m,  $\sigma_w$  increases at an average of  $1.5 \mu\text{S cm}^{-1}$  per week (Figure 5). This equates to an equivalent variation in  $S_w$  of 0.01 (when  $\sigma_w$  is assumed constant). In comparison, variations in  $S_w$  associated with ebullition events will occur abruptly producing an increase in  $\sigma(t_2)/\sigma(t_1)$ : the ratio of  $\sigma$  at time 2 to  $\sigma$  at time 1. The magnitude of this increase will depend on the ebullition dynamics of the peat core. Therefore, we focused on

investigating short-term variations in  $\sigma$  over weekly periods to ascertain whether such ebullition events can be identified, assuming that variations in  $\sigma_w$  are minimal during such short time periods.

### 6.3. E1: Spatially Explicit Measure of Ebullition Events and Bubble Movement

[31] We identified the largest ebullition events using the data from the Mariotte regulators, and identified the origin within the peat cores of these escaping bubbles. We looked at the remaining electrical images during periods where no large ebullition events occurred to characterize the movement of bubbles within the peat cores.

#### 6.3.1. Origin of Ebullition Events

[32] The six largest ebullition events during E1 gave losses of 325 to 155  $\text{cm}^3$  of gas per day per core (0.021 to 0.0099  $\text{m}^3$  of gas per day per  $\text{m}^3$  of peat; 0.0103 to 0.0049  $\text{m}^3$  of gas per day per  $\text{m}^2$ ). The ratio inversions across these ebullition events are presented in Figure 6. During these ebullition events, the images show no clear region of increased  $\sigma(t_2)/\sigma(t_1)$  (Figure 6). The lack of a substantial change of  $\sigma(t_2)/\sigma(t_1)$  suggests that the ebullition events are not associated with a loss of entrapped gas from discrete and relatively small regions within the peat cores; i.e., they are not associated with the loss of a single large entrapped gas bubble or loss from a discrete zone in the peat with a high gas content. As noted earlier, such a significant increase in  $S_w$  from a small zone would be clearly identifiable within the electrical images. Instead, the lack of substantial change in  $\sigma(t_2)/\sigma(t_1)$  anywhere in the cores strongly suggests the escaping gas originated from multiple locations across the peat cores (it had a spatially diffuse origin). It suggests either that a number of smaller, independent, spatially distributed, ebullition events occurred over a short time period (<24 h) or, more likely, that instabilities associated with one ebullition event and/or the coalescence of biogenic gas bubbles within that ebullition event caused the movement of a number of small accumulations from different locations throughout the peat core. For example, within the *S. pulchrum* peat core 10, a single large ebullition event of 230  $\text{cm}^3$  was identified from

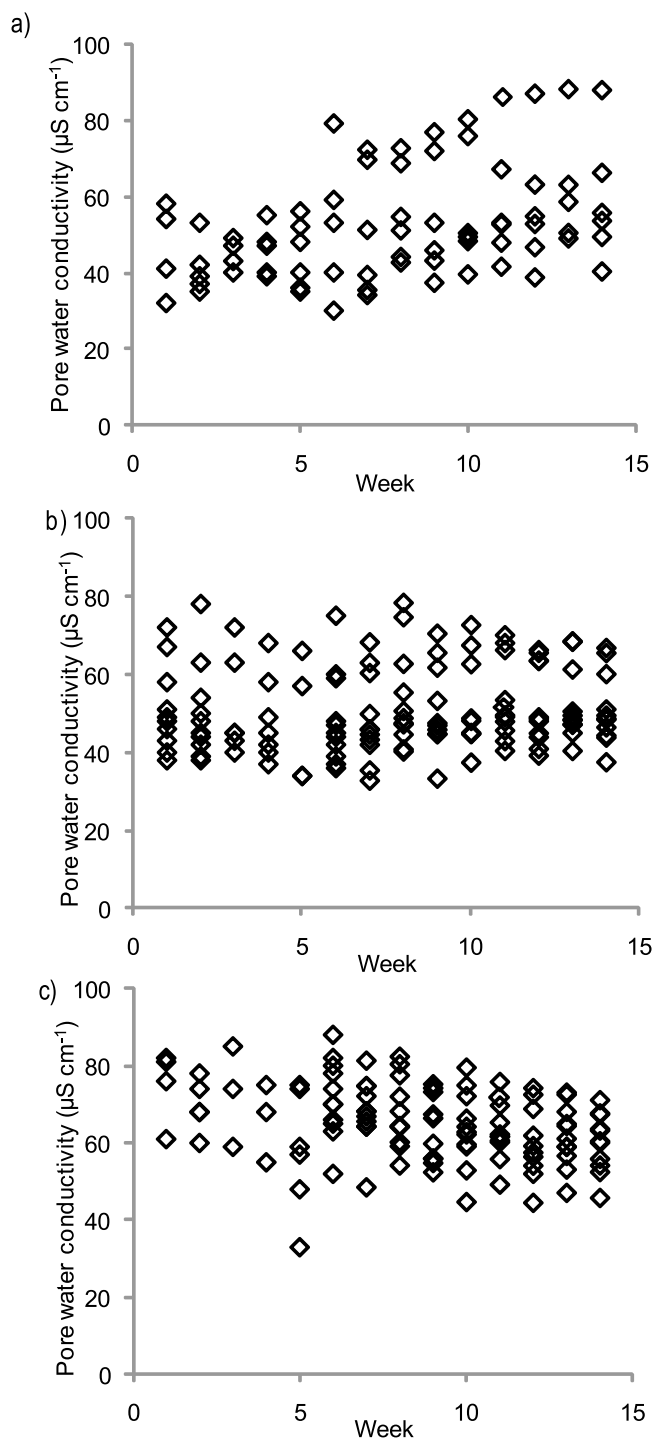


**Figure 5.** Measured pore water conductivities from all peat cores at a depth of (a) 0.07, (b) 0.14, and (c) 0.30 m, respectively.

the Mariotte regulators. However, only a small increase in  $\sigma(t_2)/\sigma(t_1)$  was identifiable at a height of 0.25 to 0.45 m from the base of the sample (Figure 6c). While small, this increase in  $\sigma(t_2)/\sigma(t_1)$  can explain the ebullition event recorded by the Mariotte regulator. Assuming a degree of saturation of 0.95 and a porosity of 0.95, an ebullition event of this magnitude occurring across the peat core from a height of 0.25 to 0.45 m from the base of the sample, would

equate to the measured increase in  $\sigma(t_2)/\sigma(t_1)$  above the lower peat of 0.024.

### 6.3.2. Movement of Bubbles Within Peat Core

[33] While  $\sigma(t_2)/\sigma(t_1)$  remains relatively constant during the large ebullition events, variations in  $\sigma(t_2)/\sigma(t_1)$  are evident when no large ebullition event is observed. These variations in  $\sigma(t_2)/\sigma(t_1)$  suggest a movement of biogenic gas bubbles or small losses of entrapped gas via ebullition that are not detected by the Mariotte regulators [cf. Green and Baird, 2011].

[34] Of particular interest is a period of falling atmospheric pressure during experiment 1 between weeks 5 and 6 (i.e., during the period of summer conditions). In the first five weeks of the incubation the atmospheric pressure rose gradually from 1004 to 1045 hPa (Figure 7). It then dropped to 1009 hPa over the course of five days. This drop was accompanied by several ebullition events recorded by the Mariotte regulators (see Green and Baird, unpublished manuscript). For the four *S. pulchrum* peat samples (cores 7–10), 35 cm<sup>3</sup> of gas was lost from sample 7 in several small events, no gas was lost from samples 8 and 9, and 230 cm<sup>3</sup> was lost from sample 10 in a single event (as discussed above). The electrical imaging results for these peat samples are presented in Figure 8 and Figure 6c. As highlighted above, while a large ebullition event was measured from *S. pulchrum* sample 10, the change in conductivity remained relatively uniform throughout, with only a small increase in  $\sigma(t_2)/\sigma(t_1)$  at a height of 0.25 to 0.45 m from the base of the sample. In comparison, within samples 7 and 8, large increases in  $\sigma(t_2)/\sigma(t_1)$  of up to 1.1 are clearly identifiable at a height of 0.35 to 0.4 m and 0.3 to 0.4 above the base of the sample, respectively (Figures 8a and 8b). It is unclear whether these (and other such) increases in  $\sigma$ , are the result of ebullition events or the redistribution of entrapped gas within the peat core. Although the increases in  $\sigma(t_2)/\sigma(t_1)$  were greater in cores 7 and 8 than in core 10, these increases in the entrapped gas content occurred within a much smaller volume of the peat core. The total gas lost may therefore be too small to be clearly identified from the Mariotte regulators (see Green and Baird, unpublished manuscript). If the volume of gas is too small to be identified confidently from the Mariotte regulators, the redistribution of a small volume of gas can only be verified by identifying an associated zone of decreased  $\sigma$  where the gas becomes re-entrained within the peat. Such regions are not evident within the core 7 and 8 during the period of pressure drop. In addition, the identified increases in  $\sigma$  occurred close to the peat surface suggesting that the gas would have left the core as a small ebullition event. In comparison, Core 11, in week 11 (Figure 9) shows a clear region of increased conductivity at a height of 0.25 to 0.35 m above the base of the peat profile, and a subsequent decrease in conductivity above. This event was characterized by a small ebullition event as recorded by the Mariotte regulators (35 cm<sup>3</sup>), which suggests that much of the gas lost from the region of increased conductivity was redistributed within the peat core.

[35] During the atmospheric pressure drop, unrealistic values of  $\sigma(t_2)/\sigma(t_1)$  occurred within *S. pulchrum* core 10, ranging from 0.2 to 10.0, which cannot be accounted for from changes in  $S_w$  associated with ebullition events. Assuming  $S_w$  equal to 0.95, changes in the degree of

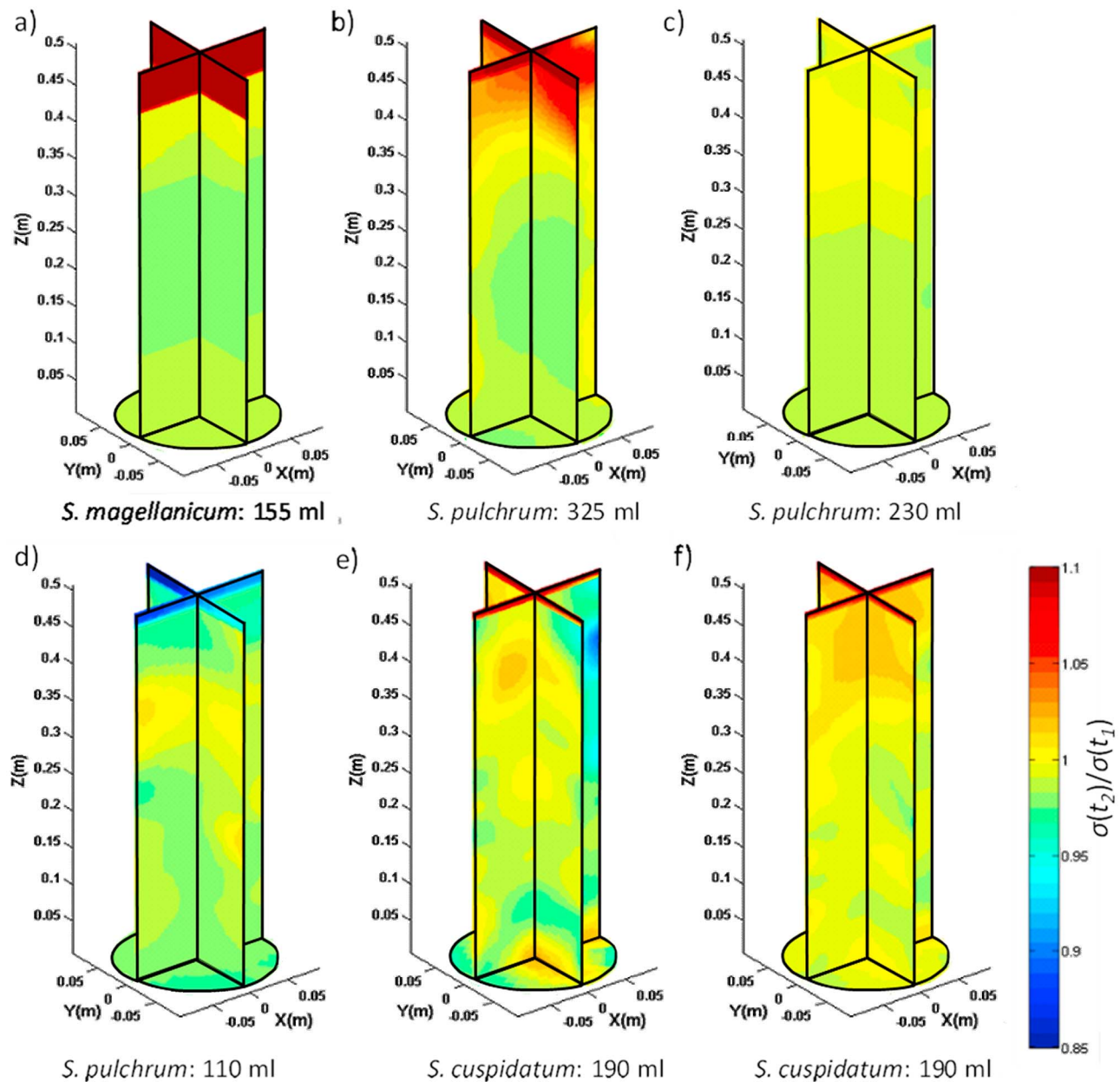


**Figure 6.** Measurements of  $\sigma(t_2)/\sigma(t_1)$  obtained during the largest ebullition events identified during experiment 1 from the Mariotte regulators. The peat type and size of the ebullition event is indicated beneath each panel (a–f).

saturation of  $\pm 1.0$  would be required to account for the measured  $\sigma(t_2)/\sigma(t_1)$  within core 3 (Figure 8c). Although not unique, the occurrence of such events were limited, occurring only twice in all cores during E1. These large alterations to  $\sigma$  do not appear to be associated with erroneous resistance measurements. The reciprocal errors during these measurement periods are not substantially greater than those measured during other periods and from other cores. The exact cause of such a shift in  $\sigma$  therefore remains unclear, although a plausible explanation is that these measured variations in  $\sigma$  are associated with the redistribution of biogenic gas bubbles within the peat core during pressure changes.

[36] If this movement of entrapped gas occurs in close proximity to the electrodes (the annular interface between the peat and the PVC column may enhance such movement) the inverted image may not provide a realistic representation of  $\sigma(t_2)/\sigma(t_1)$ . Trapped gas bubbles in close proximity to a number of the electrodes cannot be adequately represented within the ratio inversion. The elements in the finite element mesh used to represent current flow through the peat core have a volume of  $0.61 \text{ cm}^3$ . If such gas bubbles interfere with the current flow around a number of electrodes, the buildup of gas along the annular interface may be represented within the inversion by unrealistic alterations to the simulated  $\sigma$  distribution. While this problem may

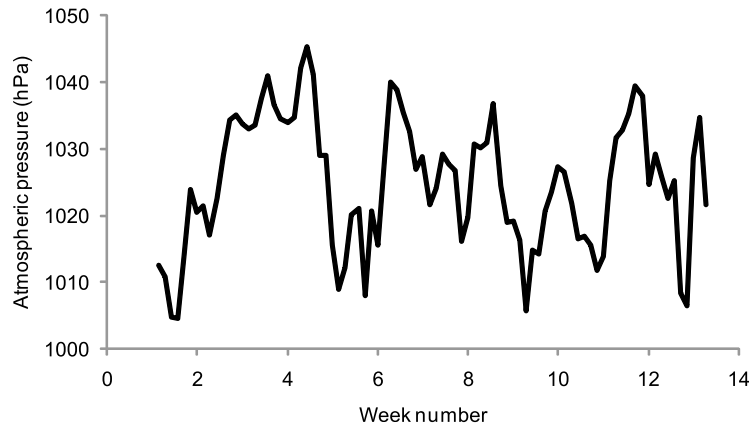


**Figure 7.** Atmospheric pressure measured over the first 14 weeks of experiment 1.

prevent the size or location of ebullition events from being properly represented, it does suggest movement of biogenic gas bubbles within the peat core and thus a relatively dynamic system. This is evident in E2 where core 28 had unrealistically high and low  $\sigma(t_2)/\sigma(t_1)$  every week. In comparison, all other cores had realistic values in the range 0.95 to 1.05, suggesting that there was more movement of gas bubbles within core 28 than the other 9 cores. This observation is confirmed by the substantially greater ebullition losses from core 28 (as recorded by the Mariotte regulators) which were in total 1.7 times larger than those of the core with the second highest ebullition flux and 5.4 times the average ebullition flux from the other nine peat cores in E2.

#### 6.4. E1 and E2: Effect of Meteorological Conditions, Peat Type, and Vascular Plant Cover on Bubble Dynamics

[37] Characterization of individual ebullition events using electrical imaging has been shown above to be problematic. Large events can be associated with only small variations in  $\sigma(t_2)/\sigma(t_1)$  over large regions of the peat core, while small ebullition events or movements of entrapped gas can produce large variation in  $\sigma$ . In addition, it appears possible that small-scale alterations to the current flow around the measurement electrodes may produce electrical images that are

not representative of the detailed distribution of entrapped gas content through the peat profile. Although the determination of individual ebullition events may not be feasible, a measurement of the degree of “roughness” of the electrical images (the variation in the degree of  $\sigma$  between adjacent voxels) does provide a measure of the internal bubble dynamics of the peat cores. The loss or movement of entrapped gas within a sample will produce a change in  $\sigma(t_2)/\sigma(t_1)$ . A region from which gas is lost will show values less than 1.0 and regions where gas is gained will show values greater than 1.0. Excluding the larger, spatially distributed, ebullition events discussed above, the movement of entrapped gas within and from the peat cores, will produce abrupt changes in  $\sigma(t_2)/\sigma(t_1)$  and, therefore, a rough spatial texture in  $\sigma(t_2)/\sigma(t_1)$ . In comparison, changes in  $\sigma(t_2)/\sigma(t_1)$  associated with variations in the pore water electrical conductivity will produce spatially smooth images. We used a measure of the image roughness ( $R$ ) to identify whether the internal bubble dynamics vary significantly between different meteorological conditions, peat types, and between cores with and without vascular plants.  $R$  is defined as

$$R = \frac{1}{NM} \sum_{i=1}^N \sum_{k=1}^M (\sigma_{r,i} - \sigma_{r,k})^2, \quad (3)$$

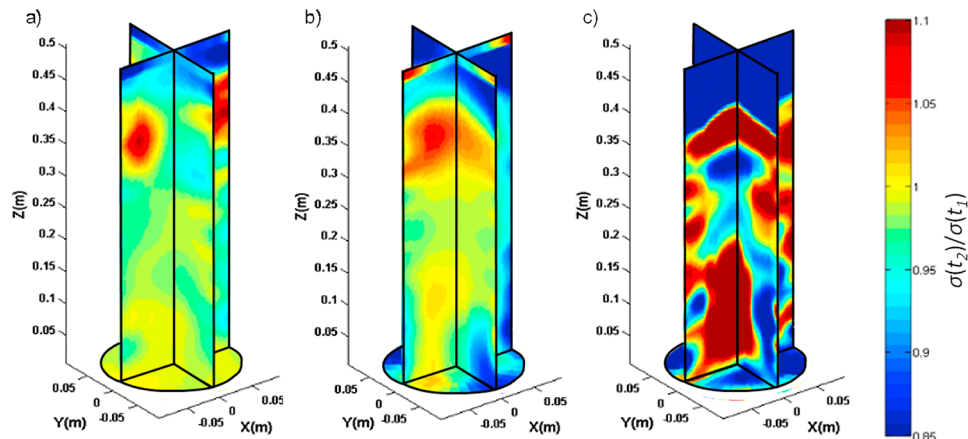


**Figure 8.** Measurements of  $\sigma(t_2)/\sigma(t_1)$  obtained from *S. pulchrum* samples (a) 7, (b) 8, and (c) 10 during the period of atmospheric pressure drop between weeks 4 and 5.

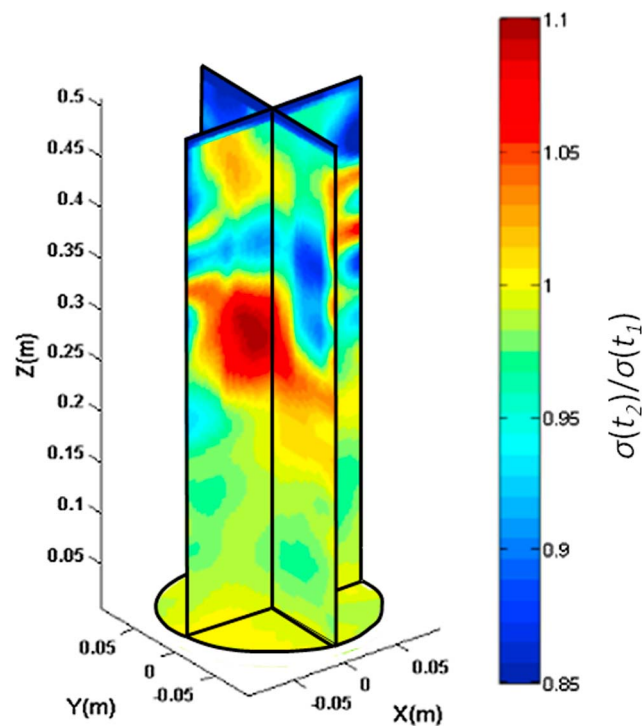


**Figure 9.** Measurements of  $\sigma(t_2)/\sigma(t_1)$  obtained from *S. cuspidatum* sample 11 during week 11.

where  $\sigma_{r,i}$  represents  $\sigma(t_2)/\sigma(t_1)$  in voxel  $i$  ( $i = 1, 2, \dots, N$ ) and  $\sigma_{r,j}$  represents  $\sigma(t_2)/\sigma(t_1)$  in the  $M$  voxels that are horizontally adjacent to voxel  $i$ . The larger the value of  $R$ , the greater the contrast between horizontally adjacent voxels (i.e., greater heterogeneity in changes in bulk conductivity) and hence apparent roughness of the image.

#### 6.4.1. Meteorological Conditions

[38] The roughness of the electrical images of the *S. magellanicum*, *S. pulchrum* and *S. cuspidatum* peat cores varied significantly between the different seasons ( $p < 0.001$ ) (Figure 10a). Under warmer summer conditions,  $\sigma(t_2)/\sigma(t_1)$  was rougher, suggesting greater movement of biogenic gas bubbles within the peat cores. This is consistent with the ebullition events measured from the Mariotte regulators which show a higher rate of ebullition from the peat cores during the warmer summer conditions (Green and Baird, unpublished manuscript). It seems that the small decrease in the peat temperatures of 3°C between summer and early autumn, and the associated decrease in  $\text{CH}_4$  production [Dunfield et al., 1993] and increases in  $\text{CH}_4$  solubility, were sufficient to change significantly the peat's internal bubble dynamics.

#### 6.4.2. Peat Type

[39] During the warmer summer period, the roughness of the electrical images does not vary significantly with peat type ( $p > 0.05$ ) (Figure 10b). Under these warmer conditions, differences in the peat type do not appear to have a significant control on the mobility of entrapped gas within the peat cores. In comparison, during the cooler autumn period, the roughness of the electrical images varies significantly ( $p < 0.01$ ) between the different peat types. During these cooler conditions,  $\sigma(t_2)/\sigma(t_1)$  is roughest within the *S. cuspidatum* cores, followed by the *S. pulchrum* cores,

with *S. magellanicum* cores showing the smoothest spatial distribution in  $\sigma(t_2)/\sigma(t_1)$  (Figure 10c). Far fewer ebullition events were identified from the Mariotte regulators during this cooler period, and the smoother distributions of  $\sigma(t_2)/\sigma(t_1)$  suggest a smaller internal movement of entrapped gas through the peat cores during this time. It appears that the structure of the peat has a more important control on the buildup, internal movement and loss of biogenic gas bubbles when the system is less dynamic.

#### 6.4.3. Vascular Plant Cover

[40] The roughness of the electrical images does not vary significantly between those peat cores with and those without a sedge vascular vegetation cover under either shaded or unshaded conditions ( $p > 0.05$ ) (Figure 10d). This finding is in agreement with the ebullition events identified from the Mariotte regulators that showed no significant variation in the  $\text{CH}_4$  loss via ebullition under the different vascular vegetation covers [Green and Baird, 2011].

## 7. Conclusions

[41] We have shown the potential and the limitations of applying electrical imaging to monitor the bubble dynamics of peat cores. When pore water conductivities are low, difficulties in characterizing the 1-D, and potentially 3-D, spatial variation in the pore water conductivity can make the characterization of the spatial distribution in the entrapped gas content difficult. However, the electrical imaging approach does have potential both under laboratory and field conditions, notably at identifying the loss of bubbles during large ebullition events by looking at changes in the bulk electrical conductivity of the peat over short time periods. We have shown how it is possible to identify individual ebullition events by looking at spatial and temporal variations in  $\sigma(t_2)/\sigma(t_1)$ . This approach is not without difficulty; the movement of entrapped gas bubbles around the electrodes during periods of ebullition may be responsible for apparently unrealistic values of  $\sigma(t_2)/\sigma(t_1)$ . However, during the largest ebullition events recorded during the study period,  $\sigma(t_2)/\sigma(t_1)$  remained relatively uniform throughout the peat cores. This strongly suggests that these larger ebullition events are spatially diffuse in terms of where the escaping bubbles originate in the peat. There is also strong evidence to suggest that discrete pockets of bubbles move through the peat profile.

[42] We quantitatively analyzed the roughness of the electrical images and used this to characterize the movement of entrapment biogenic gas bubbles. While large ebullition events were associated with smoothed spatial distributions of  $\sigma(t_2)/\sigma(t_1)$ , smaller ebullition events, or transfers of entrapped gas within the peat column, resulted in distinct intracore variations in  $\sigma(t_2)/\sigma(t_1)$ . We show that this roughness of  $\sigma(t_2)/\sigma(t_1)$  varies significantly between season and between peat type but not between cores with and without a sedge vascular plant cover. This shows that small variations in the peat temperatures can have a significant influence on the internal ebullition dynamics in peat. In addition, it shows that variations in peat between different microhabitats can significantly influence the internal ebullition dynamics. These differences in the gas entrapment between peat types at low temperatures are likely to result from both differences in the porosity of the peat, and how the constituents of the peat is structurally arranged [Kettridge and Binley 2011].

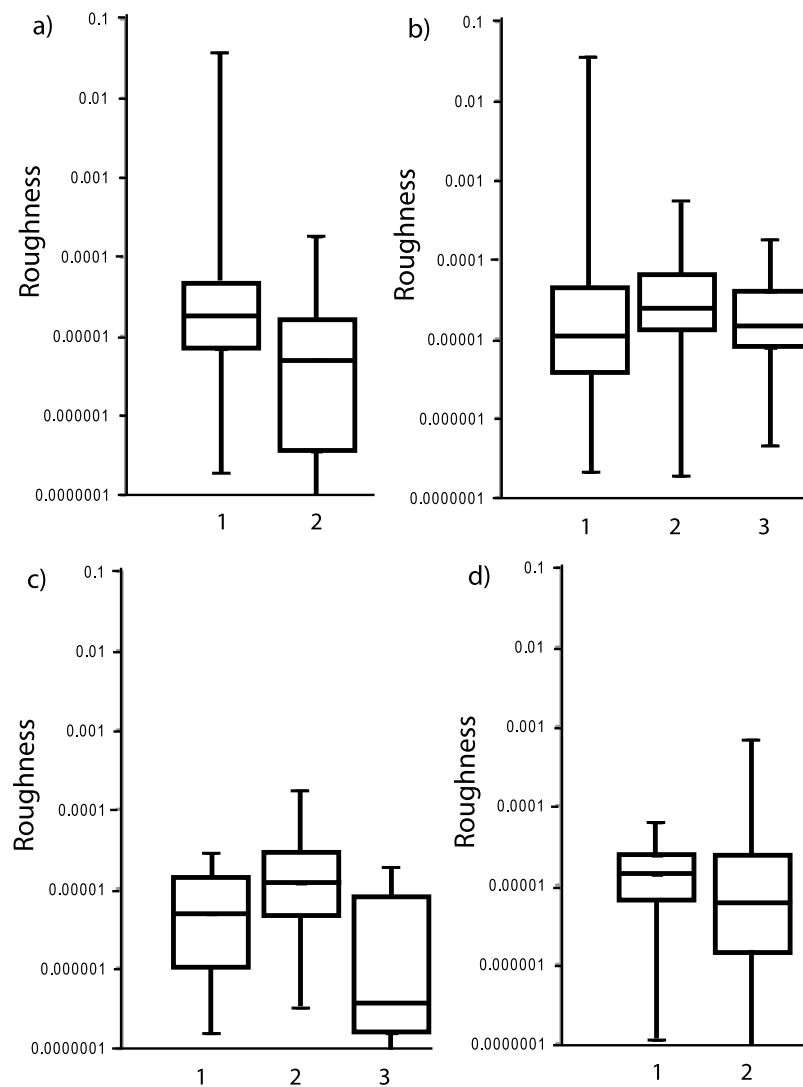


**Figure 10.** Box plots of image roughness (a) 1 = 15°C max temp, 2 = 12°C max temp; (b) max temp 15°C, 1 = *S. pulchrum*, 2 = *S. cuspidatum*, 3 = *S. magellanicum*; (c) max temp 12°C, 1 = *S. pulchrum*, 2 = *S. cuspidatum*, 3 = *S. magellanicum*; and (d) 1 = no sedge cover, 2 = high sedge cover during the second period of full light conditions.

[43] **Acknowledgments.** The authors would like to thank the Countryside Council for Wales and Scottish Natural Heritage for kindly providing access to the field sites. We are also grateful to John Kerry for the Matlab script used to visualize the electrical images. The editor, associate editor, and three anonymous reviewers are thanked for their constructive comments on a previous version of this manuscript. Financial support was provided by the UK's Natural Environment Research Council through grant NE/F004958/1.

## References

- Baird, A. J., C. W. Beckwith, S. Waldron, and J. M. Waddington (2004), Ebullition of methane-containing gas bubbles from near-surface *Sphagnum* peat, *Geophys. Res. Lett.*, *31*, L21505, doi:10.1029/2004GL021157.
- Beckwith, C. W., and A. J. Baird (2001), Effect of biogenic gas bubbles on water flow through poorly decomposed blanket peat, *Water Resour. Res.*, *37*(3), 551–558, doi:10.1029/2000WR900303.
- Binley, A., and A. Kemna (2005), DC resistivity and induced polarization methods, in *Hydrogeophysics*, edited by Y. Rubin and S. S. Hubbard, pp. 129–156, Springer, Dordrecht, Netherlands, doi:10.1007/1-4020-3102-5\_5.
- Binley, A., P. Winship, L. J. West, M. Pokar, and R. Middleton (2002), Seasonal variation of moisture content in unsaturated sandstone inferred from borehole radar and resistivity profiles, *J. Hydrol.*, *267*, 160–172, doi:10.1016/S0022-1694(02)00147-6.
- Christensen, T. R., N. Panikov, M. Mastepanov, A. Joabsson, A. Stewart, M. Öquist, M. Sommerkorn, S. Reynaud, and B. Svensson (2003), Biotic controls on CO<sub>2</sub> and CH<sub>4</sub> exchanges in wetlands—A closed environment study, *Biogeochemistry*, *64*, 337–354, doi:10.1023/A:1024913730848.
- Comas, X., and L. Slater (2004), Low-frequency electrical properties of peat, *Water Resour. Res.*, *40*, W12414, doi:10.1029/2004WR003534.
- Comas, X., and L. Slater (2007), Evolution of biogenic gasses in peat blocks inferred from noninvasive dielectric permittivity measurements, *Water Resour. Res.*, *43*, W05424, doi:10.1029/2006WR005562.
- Comas, X., L. Slater, and A. Reeve (2008), Seasonal geophysical monitoring of biogenic gasses in a northern peatland: Implications for temporal and spatial variability in free phase gas production rates, *J. Geophys. Res.*, *113*, G01012, doi:10.1029/2007JG000575.
- Coulthard, T., A. J. Baird, J. Ramirez, and J. M. Waddington (2009), Methane dynamics in peat: The importance of shallow peats and a novel reduced-complexity approach for modeling ebullition, in *Carbon Cycling in Northern Peatlands*, *Geophys. Monogr. Ser.*, vol. 184, edited by A. J. Baird et al., pp. 173–189, AGU, Washington, D. C.
- Daily, W., A. Ramirez, A. Binley, and D. LeBrecque (2004), The meter reader—Electrical resistance tomography, *Leading Edge*, *23*(5), 438–442, doi:10.1190/1.1729225.

- Dinel, H., S. P. Mathur, A. Brown, and M. Lévesque (1988), A field study of the effect of depth on methane production in peatland waters: Equipment and preliminary results, *J. Ecol.*, *76*, 1083–1091, doi:10.2307/2260635.
- Dunfield, P., R. Knowles, R. Dumont, and T. R. Moore (1993), Methane production and consumption in temperate and subarctic peat soils: Response to temperature and pH, *Soil Biol. Biochem.*, *25*, 321–326, doi:10.1016/0038-0717(93)90130-4.
- Frolking, S., N. Roulet, and J. Fuglestedt (2006), How northern peatlands influence the Earth's radiative budget: Sustained methane emission versus sustained carbon sequestration, *J. Geophys. Res.*, *111*, G01008, doi:10.1029/2005JG000091.
- Glaser, P. H., J. P. Chanton, P. Morin, D. O. Rosenberry, D. I. Siegel, O. Ruud, L. I. Chasar, and A. S. Reeve (2004), Surface deformations as indicators of deep ebullition fluxes in a large northern peatland, *Global Biogeochem. Cycles*, *18*, GB1003, doi:10.1029/2003GB002069.
- Gorham, E. (1991), Northern peatlands: Role in the carbon cycle and probable responses to climatic warming, *Ecol. Appl.*, *1*, 182–195, doi:10.2307/1941811.
- Granberg, G., H. Grip, M. Otosson Löfvenius, I. Sundh, B. H. Svensson, and M. Nilsson (1999), A simple model for simulation of water content, soil frost, and soil temperatures in boreal mixed mires, *Water Resour. Res.*, *35*(12), 3771–3782, doi:10.1029/1999WR900216.
- Green, S. M., and A. J. Baird (2011), A mesocosm study of the role of the sedge *Eriophorum angustifolium* in the efflux of methane—including that due to episodic ebullition—from peatlands, *Plant Soil*, in press, doi:10.1007/s11104-011-0945-1.
- Joabsson, A., T. R. Christensen, and B. Wallen (1999), Vascular plant controls on methane emissions from northern peatforming wetlands, *Trends Ecol. Evol.*, *14*, 385–388, doi:10.1016/S0169-5347(99)01649-3.
- Kellner, E., and L.-C. Lundin (2001), Calibration of time domain reflectometry for water content in peat soil, *Nord. Hydrol.*, *32*, 315–332.
- Kellner, E., J. S. Price, and J. M. Waddington (2004), Pressure variations in peat as a result of gas bubble dynamics, *Hydrol. Processes*, *18*, 2599–2605, doi:10.1002/hyp.5650.
- Kellner, E., A. J. Baird, M. Oosterwoud, K. Harrison, and J. M. Waddington (2006), Effect of temperature and atmospheric pressure on methane (CH<sub>4</sub>) ebullition from near-surface peats, *Geophys. Res. Lett.*, *33*, L18405, doi:10.1029/2006GL027509.
- Kettridge, N., and A. Binley (2008), X-ray computed tomography of peat soils: Measuring gas content and peat structure, *Hydrol. Processes*, *22*, 4827–4837, doi:10.1002/hyp.7097.
- Kettridge, N., and A. Binley (2010), Evaluating the effect of using artificial pore water on the quality of laboratory hydraulic conductivity measurements of peat, *Hydrol. Processes*, *24*, 2629–2640, doi:10.1002/hyp.7693.
- Kettridge, N., and A. Binley (2011), Characterization of peat structure using X-ray computed tomography and its control on the ebullition of biogenic gas bubbles, *J. Geophys. Res.*, *116*, G01024, doi:10.1029/2010JG001478.
- Koestel, J., A. Kemna, M. Javaux, A. Binley, and H. Vereecken (2008), Quantitative imaging of solute transport in an unsaturated and undisturbed soil monolith with 3-D ERT and TDR, *Water Resour. Res.*, *44*, W12411, doi:10.1029/2007WR006755.
- LaBrecque, D. J., M. Miletto, W. Daily, A. Ramirez, and E. Owen (1996), The effects of noise on Occam's inversion of resistivity tomography data, *Geophysics*, *61*, 538–548, doi:10.1190/1.1443980.
- Lansdown, J. M., P. D. Quay, and S. L. King (1992), CH<sub>4</sub> production via CO<sub>2</sub> reduction in a temperature bog: A source of <sup>13</sup>C-depleted CH<sub>4</sub>, *Geochim. Cosmochim. Acta*, *56*, 3493–3503, doi:10.1016/0016-7037(92)90393-W.
- Öquist, M. G., and B. H. Svensson (2002), Vascular plants as regulators of methane emissions from a subarctic mire ecosystem, *J. Geophys. Res.*, *107*(D21), 4580, doi:10.1029/2001JD001030.
- Slater, L., X. Comas, D. Ntarlagiannis, and M. R. Moulik (2007), Resistivity-based monitoring of biogenic gases in peat soils, *Water Resour. Res.*, *43*, W10430, doi:10.1029/2007WR006090.
- Strack, M., and T. Mierau (2010), Evaluating spatial variability of free-phase gas in peat using ground-penetrating radar and direct measurement, *J. Geophys. Res.*, *115*, G02010, doi:10.1029/2009JG001045.
- Strack, M., E. Kellner, and J. M. Waddington (2005), Dynamics of biogenic gas bubbles in peat and their effects on peatland biogeochemistry, *Global Biogeochem. Cycles*, *19*, GB1003, doi:10.1029/2004GB002330.
- Strack, M., E. Kellner, and J. M. Waddington (2006), Effect of entrapped gas on peatland surface level fluctuations, *Hydrol. Process.*, *20*, 3611–3622, doi:10.1002/hyp.6518.
- Ström, L., A. Ekberg, M. Mastepanov, and T. R. Christensen (2003), The effect of vascular plants on carbon turnover and methane emission from a tundra wetland, *Global Change Biol.*, *9*, 1185–1192, doi:10.1046/j.1365-2486.2003.00655.x.
- Ström, L., M. Mastepanov, and T. R. Christensen (2005), Species-specific effects of vascular plants on carbon turnover and methane emissions from wetlands, *Biogeochemistry*, *75*, 65–82, doi:10.1007/s10533-004-6124-1.
- Thomas, K. L., J. Benstead, K. L. Davies, and D. Lloyd (1996), Role of wetlands plants in the diurnal control of CH<sub>4</sub> and CO<sub>2</sub> fluxes in peat, *Soil Biol. Biochem.*, *28*, 17–23, doi:10.1016/0038-0717(95)00103-4.
- Tokida, T., T. Miyaxaki, M. Mizoguchi, O. Nagata, F. Takakai, A. Kagemoto, and R. Hatano (2007), Falling atmospheric pressure as a trigger for methane ebullition from peatland, *Global Biogeochem. Cycles*, *21*, GB2003, doi:10.1029/2006GB002790.
- von Post, L., and E. Granlund (1926), Sodra sveriges tortillgangar I, *Arsb. Sver. Geol. Unders.*, *335*, 1–127.
- Waddington, J. M., N. T. Roulet, and R. V. Swanson (1996), Water table control of CH<sub>4</sub> emission enhancement by vascular plants in boreal peatlands, *J. Geophys. Res.*, *101*(D17), 22,775–22,785, doi:10.1029/96JD02014.
- Waddington, J. M., K. Harrison, E. Kellner, and A. J. Baird (2009), Effect of atmospheric pressure and temperature on entrapped gas content in peat, *Hydrol. Processes*, *23*, 2970–2980, doi:10.1002/hyp.7412.

A. J. Baird, School of Geography, University of Leeds, Woodhouse Lane, Leeds, West Yorkshire LS2 9JT, UK.

A. Binley and N. Kettridge, Lancaster Environment Centre, Lancaster University, Lancaster, Lancashire LA1 4YQ, UK. (kettrin@mcmaster.ca)  
S. M. Green, Department of Earth and Environmental Science, The Open University, Walton Hall, Milton Keynes, Buckinghamshire MK7 6AA, UK.